Human Molecular Genetics, 2001, Vol. 10, No. 10 **1049–1059**

Altered proteasomal function due to the expression of polyglutamine-expanded truncated N-terminal huntingtin induces apoptosis by caspase activation through mitochondrial cytochrome c release

Nihar Ranjan Jana, Evgueni A. Zemskov, Guang-hui Wang and Nobuyuki Nukina+

Laboratory for CAG Repeat Diseases, RIKEN Brain Science Institute, 2-1 Hirosawa, Wako-shi, Saitama 351-0198, Japan

Received 20 December 2001; Accepted 7 March 2001

Expansion of CAG repeats within the coding region of target genes is the cause of several autosomal dominant neurodegenerative diseases including Huntington's disease (HD). A hallmark of HD is the proteolytic production of N-terminal fragments of huntingtin containing polyglutamine repeats that form ubiquitinated aggregates in the nucleus and cytoplasm of the affected neurons. In this study, we used an ecdysone-inducible stable mouse neuro2a cell line that expresses truncated N-terminal huntingtin (tNhtt) with different polyglutamine length, along with mice transgenic for HD exon 1, to demonstrate that the ubiquitin-proteasome pathway is involved in the pathogenesis of HD. Proteasomal 20S core catalytic component was redistributed to the polyglutamine aggregates in both the cellular and transgenic mouse models. Proteasome inhibitor dramatically increased the rate of aggregate formation caused by tNhtt protein with 60 glutamine (60Q) repeats, but had very little influence on aggregate formation by tNhtt protein with 150Q repeats. Both normal and polyglutamine-expanded tNhtt proteins were degraded by proteasome, but the rate of degradation was inversely proportional to the repeat length. The shift of the proteasomal components from the total cellular environment to the aggregates, as well as the comparatively slower degradation of tNhtt with longer polyglutamine, decreased the proteasome's availability for degrading other key target proteins, such as p53. This altered proteasomal function was associated with disrupted mitochondrial membrane potential, released cytochrome c from mitochondria into the cytosol and activated caspase-9- and caspase-3-like proteases. These results suggest that the impaired proteasomal function plays an important role in polyglutamine protein-induced cell death.

INTRODUCTION

Huntington's disease (HD) is an autosomal-dominant neurodegenerative disorder caused by abnormal expansion of polyglutamine within a 350 kDa protein of unknown function called huntingtin (1). Polyglutamine expansions are also responsible for the generation of several other inherited neurodegenerative diseases, including dentatorubral pallidoluysian atrophy, X-linked spinal bulbar muscular atrophy (SBMA) and spinocerebellar ataxia (SCA) types 1, 2, 3, 6 and 7 (2–4). Neuropathologically, HD is characterized by the death of specific neuronal subpopulations predominantly in the caudate and putamen (striatum) and at the later stages of the disease in the cerebral cortex. The neuropathological changes of HD have been categorized into four grades, progressing from grade 0, in which HD brains exhibit no microscopic abnormalities, to grade 4, in which the most severe neuronal loss is observed (5).

A common feature of all the polyglutamine diseases is the formation of ubiquitin-positive neuronal intranuclear inclusions (NIIs) (6–8). The affected neurons in the brain of HD patients show NIIs containing N-terminal huntingtin fragments (9–11), and transgenic mice expressing exon 1 of the HD gene, which contains more than 115 CAG repeats, have neuronal NIIs even before they develop neurological symptoms (12). This led to the hypothesis that such NIIs are toxic and responsible for the pathology of HD. Many cellular models of HD also demonstrate the formation of both cytoplasmic and nuclear aggregates of polyglutamine proteins that are often associated with apoptotic cell death (13–16). Several independent studies have revealed that the activation of caspase-1, -3 or -8 is required for the induction of cell death by expanded polyglutamine proteins (17–20). But the mechanisms by which those caspases are activated by the expanded polyglutamine proteins are not fully understood. One report indicates that caspase-8 is activated due to its recruitment to the polyglutamine aggregates and subsequent oligomerization (19), while another suggests that mitochondrial depolarization and activation of caspase-3 are caused by longer glutamine repeat proteins (20).

The fact that the NIIs are ubiquitinated raises the possibility that the polyglutamine-expanded proteins are misfolded and become prone to aggregation, and that their failure to refold might lead to their presentation to the proteasome system.

+To whom correspondence should be addressed. Tel: +81 48 467 9702; Fax: +81 48 462 4796; Email: nukina@brain.riken.go.jp

Indeed, several recent reports suggest that NIIs in the SCA1 (21), SCA3 (22,23), SBMA (24) and HD (25) are co-localized with various chaperone and proteasome components. In the cellular model of SCA1 (26) and SCA3 (22), proteasome inhibitors have been reported to increase the aggregate formation and, in addition, the SCA1 transgenic mice lacking E6-AP ubiquitin ligase reduce the frequency of NIIs while accelerating polyglutamine-induced pathology (26).

The ubiquitin-proteasome pathway (UPP) is predominantly a non-lysosomal protein degradation mechanism responsible for the degradation of many critical regulatory proteins involved in the regulation of cell growth and differentiation, response to stress and pathogenesis of various diseases (27,28). Degradation of a protein by this pathway involves two distinct and successive steps: (i) covalent attachment of multiple ubiquitin molecules to the target protein and (ii) degradation of the targeted protein by 26S proteasome (27). 26S proteasome is a 2.1 MDa complex of which approximately 65 subunits are divided into three subcomplexes: 20S, 19S and 11S. The 20S core catalytic complex is a cylindrical stack of four seven-membered rings and is flanked on both sides by 19S regulatory complexes. Its proteolytic site (which is trypsin-like, chymotrypsin-like and post-glutamyl peptidyl hydrolytic-like) faces an interior chamber that can be entered only through pores at either end of the cylinder. Because folded proteins cannot enter this chamber, the isolated 20S complex hydrolyzes only small peptides and denatured proteins. Several recent studies have demonstrated that proteasome dysfunction induces apoptosis in various types of cells (29–33). Inhibition of proteasome function has also been reported to activate stress kinases and induce several cytosolic and endoplasmic reticulum chaperones (34,35).

In the present study, we investigated the possible role of UPP in the pathogenesis of HD by using cellular and transgenic mouse models. We show that the proteasome system is indeed involved in the degradation of polyglutamine-expanded truncated N-terminal huntingtin (tNhtt), but that the rate of degradation is inversely dependent on the glutamine-repeat length. Recruitment of proteasome components to the aggregates and the slower rate of degradation of expanded polyglutamine proteins by proteasome decrease its availability to degrade other key target proteins such as p53. The alteration of proteasomal function is also evident from the induction of 70 kDa heat-shock protein (Hsp70) due to the expression of longer polyglutamine protein. Furthermore, we show that this altered proteasomal function is associated with apoptotic cell death through the disruption of mitochondrial membrane potential and release of cytochrome c from mitochondria.

RESULTS

Proteasome recruits to the polyglutamine aggregates

Earlier we developed several stable mouse neuro2a cell lines in an inducible system that expresses tNhtt with normal (16Q) and expanded polyglutamine (60Q and 150Q) (36). These cell lines were designated HD 16Q, HD 60Q and HD 150Q, and their corresponding expressed proteins were named tNhtt-16Q, tNhtt-60Q and tNhtt-150Q. In this cellular system, both the rates of aggregate formation and cell death were dependent on polyglutamine length and inducer dose. Cell lines were differentiated and induced together for 2 days and then processed for immunofluorescence staining of proteasome components. In HD 16Q cells, the 20S proteasome component was localized diffusely both in the cytoplasm and nucleus, and expression of tNhtt-16Q protein did not alter its normal distribution (data not shown). However, in the HD 60Q and HD 150Q cell lines, upon expression of polyglutamine protein, 20S proteasome components were redistributed to the aggregates (Fig. 1A). A similar redistribution of a 19S subunit, TBP7, to the aggregates was also observed (data not shown). In both HD 60Q and HD 150Q cells, aggregates were mainly observed in the cytoplasm, and the frequency of the cells containing aggregates was ~6–8 and 80–90% in the HD 60Q and HD 150Q cells, respectively, when checked at day 3 of induction with 1 μM of ponasterone A. Multiple aggregates were observed in most of the HD 150Q cells. An approximate estimation revealed that the aggregates in 60–70% of HD 150Q cells were 20S proteasome positive at day 3 of induction. Consistent with this result, we also observed association of the 20S proteasome component with the NIIs in the brain of R6/1 transgenic mice (Fig. 1B). Immunofluorescence staining of the 20S proteasome in the brain sections of these transgenic mice further revealed that not only the large NIIs but also several small cytoplasmic aggregates were also associated with the 20S proteasome in a manner similar to ubiquitin (Fig. 1C). In brains of R6/1 transgenic mice at the age of 30–35 weeks, the 20S proteasome positive NIIs were ~50–60% of the total counted nuclei, whereas in the same mice ubiquitin-positive NIIs were ~70–80% of the total counted nuclei.

Proteasome inhibitors enhance the rate of aggregate formation

We next attempted to determine whether proteasomes are involved in the degradation of polyglutamine-expanded tNhtt. If so, treatment with a proteasome inhibitor would be expected to increase the rate of aggregate formation by preventing their degradation. As shown in Figure 2, aggregate formation due to the expression of tNhtt-60Q was dramatically upregulated by the proteasome inhibitors ALLN and lactacystin. However, these inhibitors had very little influence on the enhancement of aggregation caused by tNhtt-150Q. Treatment with leupeptin, a lysosomal protease inhibitor, had no effect on aggregate formation. Since the proteasome inhibitors ALLN and lactacystin also affected cell viability, we cannot evaluate the effect of these inhibitors on polyglutamine protein-induced cell death.

Degradation of polyglutamine protein by proteasome depends on glutamine repeat length

Since the proteasome inhibitors enhanced the rate of aggregate formation by tNhtt-60Q but not by tNhtt-150Q, we thought that a longer glutamine repeat might have an inhibitory effect on the degradation of polyglutamine protein. Degradation of a protein by a proteasome initiates with the covalent conjugation of multiple molecules of ubiquitin to the protein and altered degradation might be expected to increase its polyubiquitinated form. We therefore induced the HD 16Q, HD 60Q and HD 150Q cells for 2 days to express their respective proteins and then equal amounts of respective proteins were immunoprecipitated with GFP antibody. Blots were probed with anti-ubiquitin. As shown in Figure 3A, a massive accumulation of

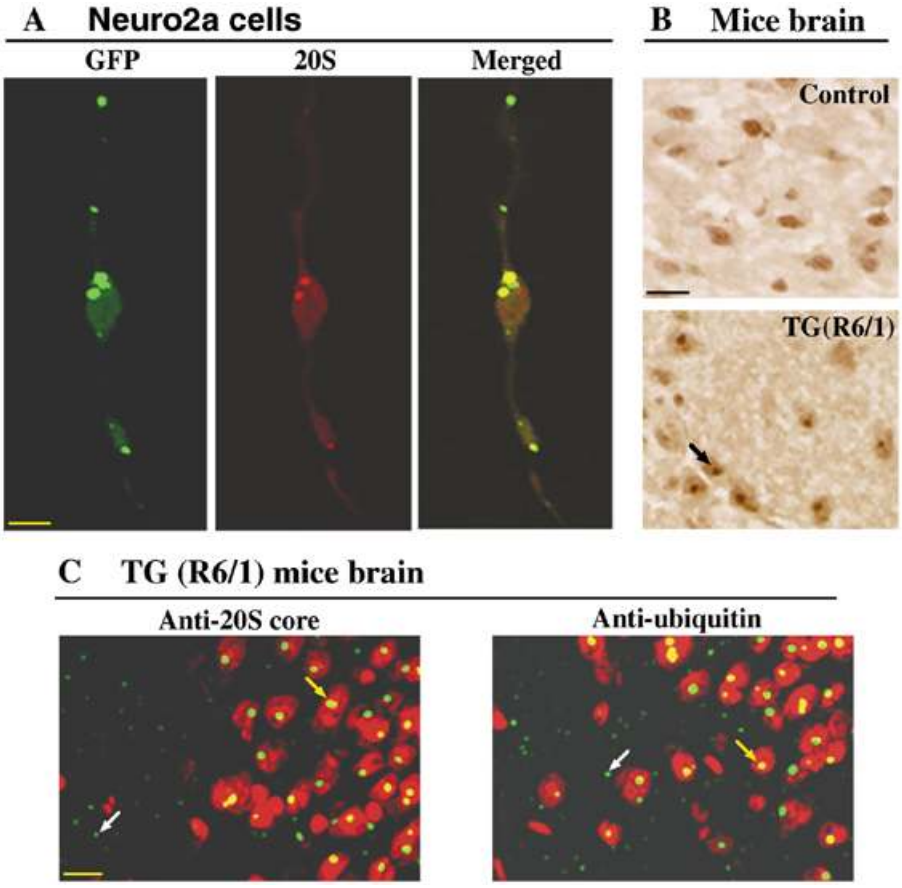

Figure 1. Proteasome 20S core component localizes to the polyglutamine aggregates. (**A**) Stable neuro2a cells expressing tNhtt-150Q were differentiated with 5 mM dbcAMP and induced with 1 μM ponasterone A for 2 days, then the cells were processed for immunofluorescence staining of 20S proteasome. CY3-conjugated (red) secondary antibody was used to label 20S proteasome. Overlay (yellow) of red signal with the green (GFP aggregate) illustrates co-localization. (**B**) Immunohistochemical staining of the 20S proteasome in the brain sections of HD exon 1 transgenic mice (R6/1 line) and their age-matched controls. The arrow indicates the NIIs stained positively with 20S proteasome. (**C**) Immunofluorescence staining of 20S proteasome and ubiquitin in the brain sections of R6/1 transgenic mice. Note the localization of 20S proteasome with small cytoplasmic (white arrows) and large nuclear aggregates (yellow arrows) in a manner similar to that of ubiquitin. Nuclei were stained by propidium iodide. Scale bars: (A) 20 μm; (B) 50 μm; (C) 10 μm.

polyubiquitin-conjugated derivatives of tNhtt-150Q proteins was observed in HD 150Q cell lines, but there was no accumulation of polyubiquitin-conjugated derivatives of either tNhtt-16Q or tNhtt-60Q proteins. Incubation of HD 150Q cell lysate with mouse IgG did not result in immunoprecipitation of either tNhtt-150Q proteins or their ubiquitinated derivatives. Figure 3B shows the same blot after probing with the N-terminal antibody of huntingtin. The tNhtt-150Q proteins appeared with two major bands, most likely because of the instability of the CAG repeat rather than the ubiquitin conjugation. In the next experiments, we induced these cell lines in the presence of 10 μM lactacystin for 24 h and then performed immunoprecipitation followed by immunoblotting with anti-ubiquitin. Accumulations of ubiquitinated derivatives were observed in all three proteins, but the accumulation of ubiquitinated derivatives of tNhtt-150Q was much higher than that of the ubiquitinated derivatives of tNhtt-16Q and tNhtt-60Q. The accumulation of ubiquitinated derivatives was more or less similar between tNhtt-16Q and tNhtt-60Q and not observed in only GFP protein (Fig. 3C). Figure 3D demonstrates the same blot after probing with anti-GFP.

Alteration of proteasomal activity by expanded polyglutamine protein

The redistribution of proteasome to the aggregates and altered degradation of soluble expanded polyglutamine protein by proteasome allowed us to investigate their impact on total cellular proteasome activity and the degradation of other proteasome substrates. We therefore induced these cell lines for different time periods, fractionated isolated cells at each time point, and proteasome activity was measured in both the soluble and precipitated fractions. The proteasome activity in the soluble fraction gradually decreased over time in ponasterone A-induced HD 150Q cells in comparison with its uninduced state, and the decrease was statistically significant at days 3 and 4 (Fig. 4A). The proteasome activity also decreased slowly over time in differentiated, but not induced, HD 150Q cells, probably due to the weak expression of tNhtt-150Q protein without induction. We have also noted that the differentiation over time increases both the level and aggregation of tNhtt-150Q (our unpublished observation). However, the proteasome activity was unaltered in HD 16Q cells upon

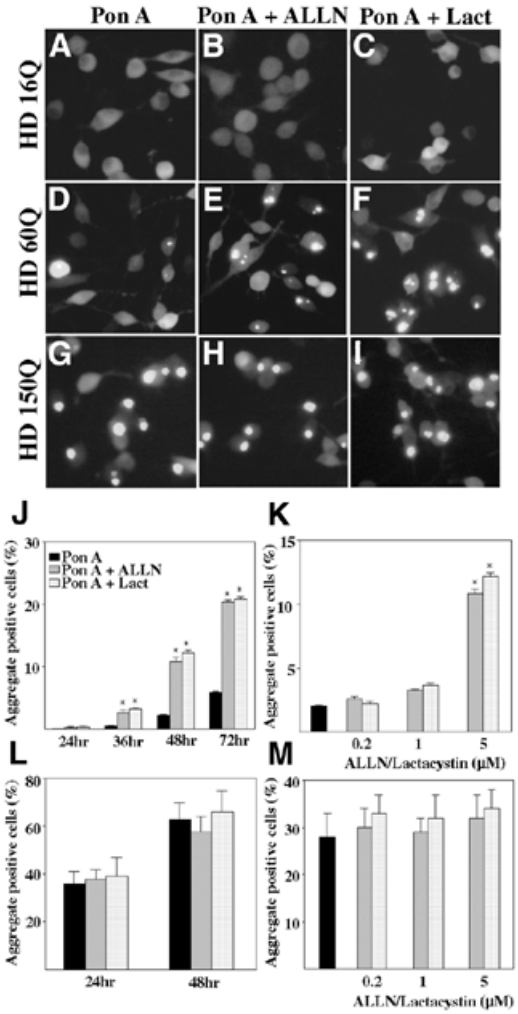

Figure 2. Proteasome inhibitors increase the rate of aggregate formation of tNhtt-60Q but not of tNhtt-150Q proteins. (Top) Differentiated HD 16Q (**A**, **B** and **C**), HD 60Q (**D**, **E** and **F**) and HD 150Q (**G**, **H** and **I**) cells were induced by 1 μM ponasterone A (pon A) in the absence (A, D and G) or presence of 5 μM of either ALLN (B, E and H) or lactacystin (C, F and I) for 48 h. The rate of aggregate formation was observed under fluorescence microscope. (Bottom) Quantitative estimation of aggregate formation in HD 60Q and HD 150Q cells. (**J** and **L**) Time-dependent effect of aggregate formation by both ALLN and lactacystin each at a dose of 5 μM in HD 60Q and HD 150Q cells, respectively. (**K** and **M**) Dose-dependent effect of aggregate formation by both ALLN and lactacystin in HD 60Q (at 48 h) and HD 150Q (at 24 h) cells, respectively. Aggregate formation was manually counted under a fluorescence microscope and the cell containing more than one aggregate were considered to have a single aggregate. Values are the means ± SD; $n = 5$. *$P < 0.001$ as compared to respective ponasterone A treated experiment.

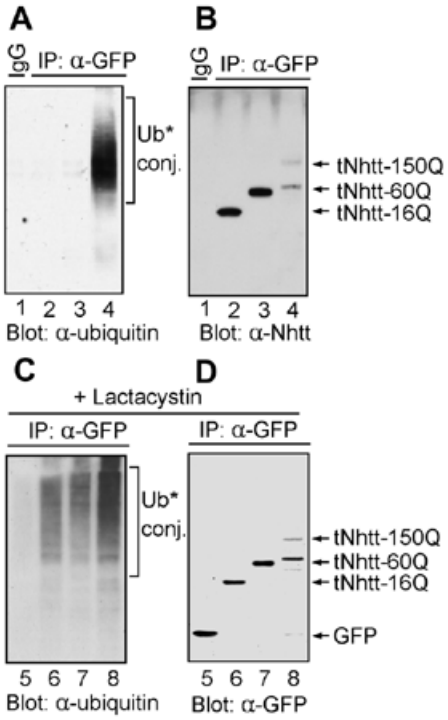

Figure 3. Ubiquitination of tNhtt. Neuro2a cells expressing tNhtt with different polyglutamine length were differentiated and induced for 2 days in the similar manner as described in Figure 1A and then processed for immunoprecipitation by GFP antibody. Blots were probed with either anti-ubiquitin (**A**) or anti-huntingtin (**B**). (**C** and **D**) Differentiated cells were induced with ponasterone A in the presence of 10 μM lactacystin for 24 h and then performed immunoprecipitation by anti-GFP. Blots were detected with either anti-ubiquitin (C) or anti-GFP (D). Lanes 1, 4 and 8, HD 150Q cell lysate; lanes 2 and 6, HD 16Q cell lysate; lanes 3 and 7, HD 60Q cell lysate; lane 5, pIND-EGFP transfected cell lysate.

induction (Fig. 4A). The proteasomal activity in the pelleted fraction of the untreated HD 150Q cells was very low (~5–6% of the total cellular proteasomal activity), but increased dramatically upon differentiation and induction of those cells (Fig. 4B). This was due to the massive formation of aggregates and association of proteasomes with the aggregates. Since we could not precisely estimate the protein concentrations in the pelleted fractions, we suspended the total pellet in 100 μl of assay buffer and used the same volume (10 μl) for the activity assay. The decrease in proteasome activity in HD 150Q cells on days 3 and 4 has correlation with cell death (Fig. 4C). The inhibition of proteasomal function has been reported to induce the expression of Hsp70 due to the accumulation of misfolded protein and, therefore, we tested the possibility that the Hsp70 is induced in our system. As shown in Figure 4D, the expression of Hsp70 was induced in both the HD 150Q and HD 60Q cells but not all detected in HD 16Q cells when they were treated with 1 μM ponasterone A for 3 days. The expression of proteins with longer polyglutamine repeats also affected the degradation of other proteasome substrates, as evidenced by the accumulation of p53 (Fig. 4D). Cycloheximide-chase experiments further confirmed that the p53 was degraded at a much slower rate in HD 150Q cells than in HD 16Q cells (Fig. 4E)

Activation of caspase-9- and caspase-3-like proteases induced by proteasomal hypofunction

Several recent reports have suggested that the expression of expanded polyglutamine protein induces apoptotic cell death, but the exact mechanism remains unclear. Consistent with these findings, we also observed nuclear fragmentation (Fig. 5A and B) and cleavage of downstream caspase substrate lamin B (Fig. 5C), a typical feature of apoptosis, in cells either

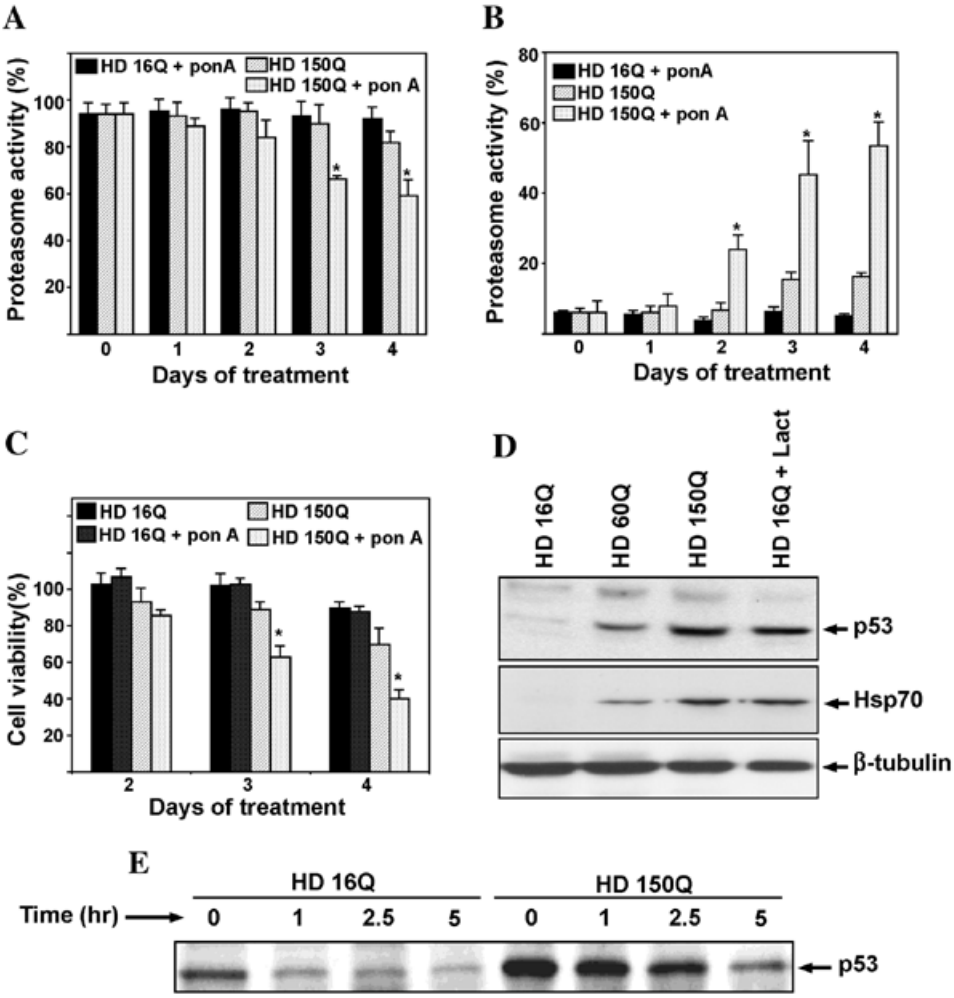

Figure 4. Alteration of proteasomal activity, heat-shock response, accumulation of p53 and cell death upon expression of polyglutamine-expanded huntingtin. (**A** and **B**) HD 16Q and HD 150Q cells were differentiated and induced for the indicated time periods and then fractionated as described in Materials and Methods. Proteasomal activity (chymotrypsin-like) was measured in both soluble (A) and precipitated fractions (B). Total proteasomal activity of the untreated wild-type or HD 150Q cells was considered as 100% and, in these cells, activity in the soluble and precipitated fractions was ~94 and 6%, respectively. Activities at all other time points in both the soluble and pelleted fractions were calculated based on these respective initial values. Equal amounts (25 µg) of protein were used for the activity assay of the soluble fractions, and an equal volume (10 µl) of suspended material was used to measure the activity in the pelleted fractions. Values are the means ± SD of five independent experiments. $*P < 0.001$ as compared to either wild-type or uninduced HD 150Q cells. (**C**) HD 16Q and HD 150Q cells were plated into 96-well tissue cultured plate, differentiated for 24 h, and then induced with 1 µM ponasterone A for the time periods indicated. The cell viability was measured by MTT assay. The cell viability of differentiated HD 16Q cells at 24 h was taken as 100%. Values are the means ± SD; $n = 4$. $*P < 0.001$ as compared to differentiated HD 150Q cells. (**D**) Cell lines were differentiated and induced for 3 days and then the total cell lysate was processed for immunoblotting by Hsp70, p53 and β-tubulin antibody. HD 16Q cells were treated with lactacystin for 24 h. (**E**) HD 16Q and HD 150Q cell lines were differentiated and induced for 2 days, then incubated for the indicated time periods in the presence of cycloheximide (10 µg/ml) and ponasterone A. Equal amounts of protein from each time point were analyzed by immunoblotting with p53 antibody.

expressing expanded polyglutamine protein or treated with lactacystin. Interestingly, however, the cells containing aggregates mostly exhibited nuclear fragmentation. The expression of longer polyglutamine repeat protein also initiated the activation of caspase-3- (Fig. 5C) and caspase-9-like proteases (Fig. 5D). This activation of caspases was most likely due to the altered proteasomal function, since the proteasome inhibitor lactacystin also initiated the activation of these caspases. Treatment with 10 µM lactacystin for 24 h caused an ~15-fold increase in caspase-3-like protease activity. Caspase-3-like protease activity was comparatively higher in uninduced HD 150Q cells, most likely because of the low levels of basal expression.

Mitochondrial dysfunction and cytochrome c release upon expression of expanded polyglutamine protein

Since the activation of caspase-9 is initiated with the release of cytochrome c from mitochondria followed by its binding to apoptosis protease activating factor-1 (Apaf-1), we further examined the effect of the expression of expanded polyglutamine protein on the disruption of mitochondrial

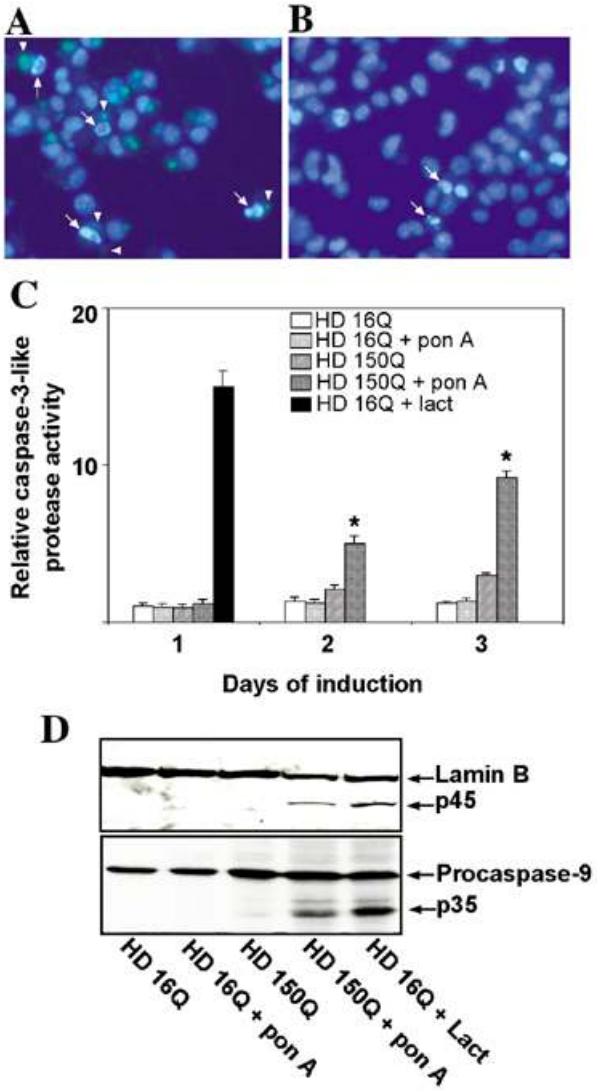

Figure 5. Expression of polyglutamine-expanded huntingtin induces cell death program. The HD 150Q cells after 72 h of differentiation and induction (**A**) and the HD 16Q cells after treatment of 10 μM lactacystin for 24 h (**B**) were stained with 50 μM Hoechst 33258 for 20 min at 37°C and then washed several times using PBS. Nuclear condensation and fragmentation were examined under a fluorescence microscope. Condensed and fragmented nuclei are indicated by arrows and polyglutamine aggregates by arrowheads. Note the cells containing aggregates undergoing nuclear fragmentation. (**C**) Caspase-3-like protease activity in the cells at the indicated time points after differentiation and induction. Values are the means ± SD of three independent experiments. $*P < 0.001$ as compared to differentiated HD 150Q cells. (**D**) Activation of caspase-9 and cleavage of lamin B. Cells were differentiated and induced for 3 days. Lactacystin was treated for 24 h.

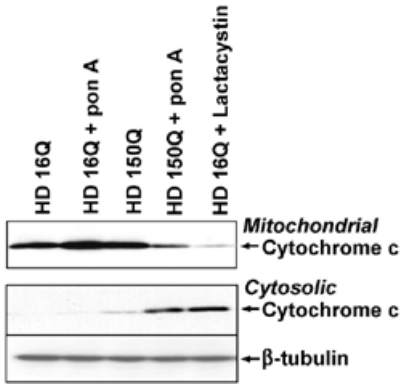

Figure 6. Release of cytochrome c from mitochondria into the cytosol upon expression of polyglutamine-expanded huntingtin. Differentiated and induced (72 h) HD 16Q and HD 150Q cells or lactacystin-treated (10 μM for 24 h) HD 16Q cells were homogenized by a Dounce homogenizer and subjected to the preparation of mitochondrial and cytosolic fractions as described in Materials and Methods. Cytochrome c was detected in both the cytosolic and mitochondrial fraction by immunoblotting. Cytosolic fractions were also probed with β-tubulin as a reference.

membrane potential and release of cytochrome c into the cytosol. As shown in Figure 6, expression of tNhtt-150Q protein for 3 days reduced the mitochondrial cytochrome c content and thereby increased the cytochrome c content in the cytosolic fraction. Expression of tNhtt-16Q protein for the same time period had no effect on cytochrome c release. Treatment of the HD 16Q cells with 10 μM lactacystin for 24 h also resulted in the release of cytochrome c from mitochondria, further suggesting that altered proteasomal function initiated by expanded polyglutamine protein might be involved at least in part in the mitochondrial cytochrome c release. However, at present, it is unknown whether the toxic effect of lactacystin is only mediated through the release of mitochondrial cytochrome c. Lactacystin might affect some other pathways of cell death signal. We next examined the alteration of mitochondrial membrane potential upon expression of expanded polyglutamine proteins. We used JC-1, a potential-sensitive fluorescent dye that detects specifically polarized mitochondria as red color, and this color shifted to diffuse green when the membrane depolarizes. Treatment of 10 μM lactacystin to the wild-type neuro2a cells dramatically disrupted mitochondrial membrane potential, as shown in Figure 7A and B. Because all of our stable cell lines also expressed GFP, we were unable to investigate the color shift with the change of mitochondrial membrane potential. We therefore observed only polarized mitochondria using 568 nm argon–krypton laser sources. Expression of tNhtt-150Q proteins for 3 days caused a frequent disappearance of red polarized mitochondria specifically in the cell containing aggregates (Fig. 7E and F). Such a phenomenon was not observed upon expression of tNhtt-16Q proteins (Fig. 7C and D), further suggesting that the disruption of mitochondrial membrane potential by expanded polyglutamine proteins is most likely due to proteasomal hypofunction.

DISCUSSION

Regulated proteolysis by UPP is crucial in controlling the intracellular levels of a variety of short-lived proteins and for maintaining cellular growth and metabolism. Altered functions of this pathway have been implicated in the pathogenesis of a number of diseases (27,28). In this study, we investigated the possible role of UPP in the pathogenesis of HD and found that impaired function of this pathway caused by polyglutamine-expanded tNhtt is one of the key factors in initiation of apoptosis.

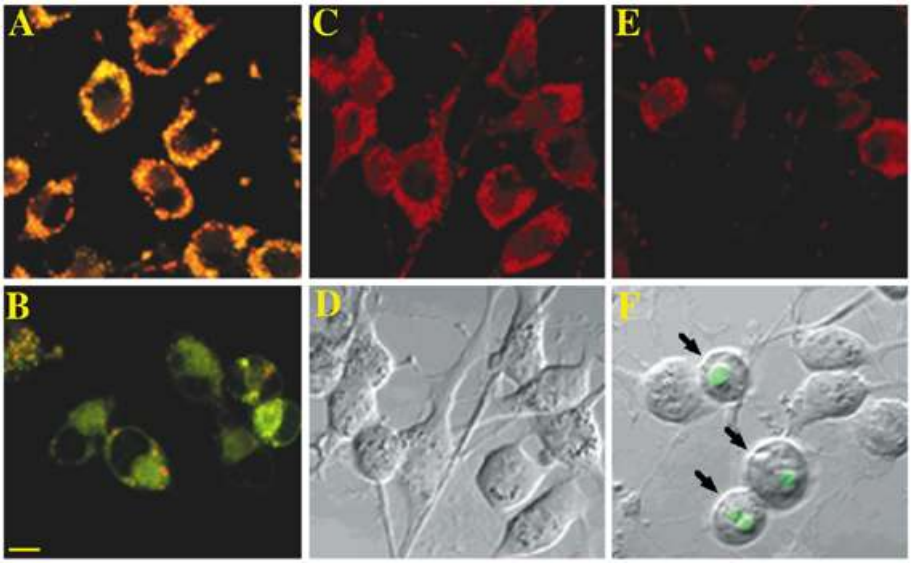

Figure 7. Changes of mitochondrial membrane potential after treatment of lactacystin or expression of polyglutamine-expanded huntingtin. Wild-type neuro2a cells were treated with either DMSO or 10 μM lactacystin for 24 h and then incubated with JC-1 as described in Materials and Methods. Change of mitochondrial membrane potential was evaluated qualitatively by observing cells under a confocal microscope. (**A** and **B**) Wild-type neuro2a cells treated with DMSO and lactacystin, respectively. The shift of red fluorescence to diffuse green indicates disruption of the membrane potential. Since all our stable cell lines expressed GFP, we evaluated the changes of mitochondrial membrane potential after expression of normal and expanded-polyglutamine huntingtin by observing polarized mitochondria (dotted red fluorescence) using 568 nm argon-krypton laser sources. (**C** and **E**) HD 16Q and HD 150Q cells, respectively, after 3 days of differentiation and induction. (**D** and **F**) The same field of HD 16Q and HD 150Q cells, respectively, under transmitted light. Note the loss of red dotted fluorescence in the HD 150Q cells containing aggregates (indicated by arrow). Scale bar; 10 μM.

First, we have shown that the proteasome components are redistributed to the polyglutamine aggregates in both cellular and transgenic mouse models of HD. Secondly, proteasome inhibitor enhances the rate of aggregate formation caused by tNhtt protein with 60Q but not by tNhtt protein with 150Q. Thirdly, a massive accumulation of ubiquitinated derivatives was observed in tNhtt protein containing 150Q, but not 60Q or 16Q. These results strongly suggest that the expanded polyglutamine proteins are degraded by proteasome, but the rate of degradation was inversely proportional to the repeat length. How polyglutamine stretch affects the degradation of mutant huntingtin is not yet clear. Ubiquitin conjugation is the first step towards the degradation of a protein by proteasome, and it seems that both normal and polyglutamine-expanded huntingtin are conjugated well with ubiquitin. The limiting steps may therefore be either substrate recognition by the 19S regulatory cap or substrate hydrolysis by the 20S catalytic core of the proteasome complex. It has been hypothesized that polyglutamine repeats that are longer than a certain critical length might be able to form a highly stable β-sheet structure by creation of a hairpin loop within the molecule (37,38). A protein substrate must need to be unfolded to gain access to enzymatic sites within the 20S catalytic core. Therefore, the domains that are resistant to unfolding may block entry into the 20S core cavity and promote the rapid release of the ubiquitinated expanded polyglutamine protein. The increase in length of the β-sheet structure due to the increasing number of glutamine might increase the resistance to unfolding. This kind of structural change from α-helix to stable β-sheet has also been proposed as a mechanism for the formation of prions (39). Alternatively, the polyglutamine domain may interfere with the targeting of ubiquitinated, expanded polyglutamine proteins to the proteasome by blocking a putative substrate-specific binding site, or by affecting the activity of molecular chaperones that may be required as an ancillary factor for the degradation of the substrate (40). A similar kind of inhibition of ubiquitin-proteasome-dependent protein degradation by the Gly–Ala repeat domain of the Epstein–Barr virus nuclear antigen-1 has been reported (41,42). Interestingly, the degradation of tNhtt with normal glutamine repeats by proteasome suggests that the normal full-length huntingtin may be the substrate of the proteasome, and that the degradation signal is located within its N-terminal [exon 1] region.

The involvement of UPP in the pathogenesis of SCA1 (21,26), SCA3 (22) and HD (25) has recently been documented. In the cellular disease model of SCA1 and SCA3, proteasome inhibitors have been shown to increase the ataxin-1 or -3 aggregation. This strongly suggests that polyglutamine-expanded proteins are the common targets of proteasome for degradation; however, the rate of degradation is dependent on the length of the glutamine repeats. Furthermore, SCA1 mutant mice lacking E6-AP ubiquitin ligase show reduced frequency of NIIs, but enhanced polyglutamine-induced pathology (26). Co-expression of a dominant-negative form of ubiquitin-conjugating enzymes with mutant huntingtin also dramatically suppressed the formation of NIIs while accelerating cell death (43). This led to the idea that the soluble form rather than the aggregated form of polyglutamine proteins is responsible for cellular apoptosis. Its remains unclear, however, whether the accelerating pathology is due to the accumulation of mutant polyglutamine proteins or accumulation of other substrates of UPP. Because p53 is shown to be upregulated in mice lacking E6-AP

ubiquitin ligase (44), and because p53 is proapoptotic (45), its altered turnover might contribute to the accelerated SCA1 pathology.

In contrast to those observations, our results suggest that polyglutamine aggregates are indeed involved in the initiation of the cell death process. First, we observed that redistribution of proteasome complex to the polyglutamine aggregates over time causes a decrease in the level of proteasomal activity in the overall cellular environment, and an increase in the aggregates. The accumulation of p53 and induction of hsp70 upon expression of expanded-polyglutamine protein further supports the proteasomal malfunction. The slower degradation of longer polyglutamine protein could be another reason for the accumulation of proapoptotic protein p53. Secondly, the proteasomal hypofunction is associated with the disruption of mitochondrial membrane potential, release of cytochrome c into the cytosol, activation of caspase-9- and caspase-3-like proteases and finally cell death. It has long been known that the inhibition of proteasomal function triggers programmed cell death depending on the cell types and condition, though the precise mechanism of cell death is still controversial (29–33). There are reports which suggest that proteasomal hypofunction induces cytochrome c release and activation of caspase-3-like proteases (32), while others suggest the involvement of p53/Bax (31,46) in the induction of apoptosis. UPP plays a vital role in the degradation of many key regulatory proteins that are necessary for cell growth and differentiation. Therefore, it is not surprising that altered degradation of those regulatory proteins will affect the cell's survival. Some proteins that are able to promote apoptosis are known to be substrates of UPP, such as p53, Bax or Bid, and these proapoptotic proteins have been reported to induce cytochrome c release from mitochondria (47,48). Once cytochrome c is released into the cytosol, it could bind with Apaf-1 and trigger the sequential activation of caspase-9 and -3 (49,50). Caspase-3 is involved in the final execution by cleaving of a variety of target proteins (51). The fact that the treatment of caspase inhibitor or overexpression of Bcl2/BclxL significantly protects against the polyglutamine-induced cell death, as observed by ourselves and others (19,43), further suggests involvement of mitochondria in the polyglutamine protein induced cell death process. Moreover, the finding of mitochondrial dysfunction in the HD brain (52,53) and glutamine repeat-length-dependent mitochondrial depolarization and subsequent activation of caspase-9 and caspase-3 in lymphoblasts derived from HD patients (20), strongly support our observations of altered proteasomal function caused by expression of polyglutamine-expanded proteins. However, the involvement of p53 in the polyglutamine protein-induced cell death remains to be clarified, because polyglutamine-expanded tNhtt has also been reported to interact with p53 and represses p53-dependent transcription (54).

Surprisingly, the transgenic mice containing the full-length HD gene with either 48 or 89 CAG repeats did show signs of apoptotic cell death (55), whereas the mice transgenic for HD exon 1 with either 100 or 150 CAG repeats did not show any sign of apoptotic cell death when they showed severe HD symptoms (12,56,57). However, inhibitor of caspases (17,18) or stabilizer of the mitochondrial permeability transition (58) significantly improved the survival of HD exon 1 transgenic mice with 150 CAG repeats, suggesting that caspases are indeed activated in these mice but may be at chronic sublethal level, and that the mitochondria are affected but not so severely. Based on our results, we assume that the misfolded full-length huntingtin was effectively targeted by the proteasome for degradation in the cytoplasm, and because of the slower degradation rate or resistance to degradation, it may have tied up proteasome activity. Furthermore, a comparatively high level expression of the full-length HD transgene due to CMV promoter possibly accelerated the proteasomal hypofunction. On the other hand, N-terminal truncated fragments could escape from the cytoplasmic proteasome barrier to gradually accumulate and form aggregates inside the nucleus. Since the nucleus is less efficient than the cytoplasm in refolding or degrading misfolded proteins, it might favour the aggregation process (59). Several nuclear factors, such as TATA-binding protein (59), CREB-binding protein (54,60) and nuclear receptor co-repressor (61), could also participate in the aggregation process, and their imbalance over time could conceivably cause neuronal dysfunction.

Altered proteasomal function has also been reported to induce the expression of several cytoplasmic heat-shock chaperones and ER-resident chaperones, and to activate stress-activated protein kinase (SAPK) as a result of the accumulation of misfolded and polyubiquitinated proteins (34,35,62,63). A very high level of induction of Hsp70 reported here and the activation of SAPK due to the expression of polyglutamine-expanded protein reported previously (64,65) further suggest altered proteasomal function in the polyglutamine diseases.

MATERIALS AND METHODS

Mice

Heterozygous HD exon 1 transgenic male mice of the R6/1 (CAG repeat no. 115) line were obtained from The Jackson Laboratory (Jackson code: B6CBA-TgN [Hdexon1]61) and maintained by crossing carrier males with CBA females. The genotyping and CAG repeat sizing were carried out using a PCR assay and Genescan, respectively, as described previously (56). Mice (transgenic and their age-matched controls) at 30–35 weeks of age were killed using ether anesthesia, and their brains carefully removed and collected in Tissue-Tek (Sakura Finetek), frozen with powdered solid CO_2 and stored in –80°C.

Antibodies

Antibodies utilized in this study were purchased from the following sources. The mouse monoclonal α-p53 (SPA-400) and α-Hsp70 (SPA-810) were from StressGen Biotechnologies. Rabbit polyclonal α-ubiquitin was from Dako, mouse monoclonal α-caspase-9 was from MBL, mouse monoclonal α-GFP and α-tubulin were from Boehringer Mannheim and mouse monoclonal α-cytochrome c was from Pharmingen. Goat polyclonal α-Lamin B (SC-6217) was from Santa Cruz Biotechnology. Rabbit polyclonal proteasome 20S core and TBP7 antibody were from Affinity Research Product. Goat anti-rabbit IgG-CY3 (Molecular Probes) was utilized as a secondary antibody in indirect immunofluorescence. HRP-conjugated anti-mouse IgG, anti-rabbit IgG (both from Amersham Life Science) and anti-goat IgG (Santa Cruz

Biotechnology) were utilized as secondary antibodies in immunoblotting.

Expression plasmids and stable cell lines

The enhanced green fluorescence protein (EGFP) and tNhtt expression constructs, pIND-EGFP, pIND-tNhtt-EGFP-16Q, pIND-tNhtt-EGFP-60Q and pIND-tNhtt-EGFP-150Q, and the generation of stable cell lines of these constructs, have been described previously (36). Each construct contains 1–90 amino acids of tNhtt (predicted molecular weight 7.8 kDa) with different polyglutamine length fused to the N-terminus of EGFP.

Cell culture, treatments and viability assay

Stable mouse neuro2a cell lines expressing tNhtt-EGFP-16Q, tNhtt-EGFP-60Q and tNhtt-EGFP-150Q were regularly maintained in DMEM (Life Technologies) supplemented with 10% FBS, 0.4 mg/ml Zeocin and 0.4 mg/ml G418. Cells were routinely differentiated by treatment with 5 mM dbcAMP (*N*6,2′-*O*-dibutyriladenosine-3′:5′-cyclic monophosphate sodium salt; Nacalai Tesque) and induced with 1 μM ponasterone A (Invitrogen). For proteasome inhibition experiments, cells (1×10^3 cells/well of the chamber slide) were treated with different doses of either lactacystin (Calbiochem) or ALLN (Affinity Research Product) for different time periods. Cell viability (5×10^3 cells/well of 96-well plate) was determined using MTT assay as described previously (36). For nuclear staining, cells were incubated with 25 μM Hoechest 33258 (Molecular Probes) for 20 min at 37°C, washed with PBS and then observed by fluorescence microscope (Olympus Opticals) at Ex/Em: 352/461 nm.

Cycloheximide-chase experiment

The stable cell lines, HD 16Q and HD 150Q were differentiated and induced simultaneously for 48 h. Cells were then washed several times with normal cultured medium and chased in the presence of 10 μg/ml cycloheximide and ponasterone A for the time periods indicated. Cells collected at each time point were then processed for immunoblotting by anti-p53.

Coimmunoprecipitation and immunoblotting experiment

Cells were washed with cold PBS, scraped, pelleted by centrifugation and lysed on ice for 30 min with RIPA buffer (10 mM HEPES pH 7.4, 150 mM NaCl, 10 mM EDTA, 2.5 mM EGTA, 1% Triton X-100, 0.1% SDS, 1% sodium deoxycholate, 10 mM NaF, 5 mM $Na_4P_2O_7$, 0.1 mM Na_2VO_5, 1 mM PMSF, 0.1 mg/ml aprotinin). Cell lysates were briefly sonicated, centrifuged for 10 min at 15 000 *g* at 4°C and the supernatants (total soluble extract) were used for immunoprecipitation. Protein concentration was measured according to the method of Bradford using Bio-Rad Protein Assay reagent (Bio-Rad Laboratories) and BSA as a standard. For each immunoprecipitation experiment, 200 μg protein in 0.2 ml RIPA buffer was incubated either with 5 μl (2 μg) of GFP antibody or 4 μl (2 μg) of normal mouse IgG. After 5–6 h of incubation at 4°C with rotation, 10 μl of magnetic protein G beads (Perspective Biosystem) were added and incubation was continued at 4°C overnight. The beads were pulled down with a magnet (Dynal) and washed six times with RIPA buffer. Bound proteins were eluted from the beads with 1× SDS sample buffer, vortexed, boiled for 5 min, and analyzed by immunoblotting. The total cell lysate or the immunoprecipitated proteins were separated through SDS–PAGE and transferred onto PVDF membranes (Immobilon-P; Millipore). The membranes were successively incubated in blocking buffer [5% skim milk in TBST (50 mM Tris pH 7.5, 0.15 M NaCl, 0.05% Tween)], with primary antibody in TBST, and then with secondary antibody conjugated with HRP in TBST. Detection was carried out with enhanced chemiluminescence reagent (Amersham Life Science).

Immunofluorescence and immunohistochemical techniques

Cells grown in chamber slides were differentiated and induced together for 2 days. Cells were washed twice with PBS, fixed with 4% paraformaldehyde in PBS for 20 min, permeabilized with 0.5% Triton X-100 in PBS for 5 min, washed extensively and then blocked with 5% non-fat dried milk in TBST for 1 h. Primary antibody incubation was carried out overnight at 4°C. After several washings with TBST, cells were incubated with the appropriate secondary antibody for 1 h, washed several times and mounted in antifade solution (Vecashield Mounting Media, Vector Laboratories). The primary antibodies, proteasome 20S core and TBP7 were used in 1:1000 dilution and the appropriate secondary antibody conjugated with CY3 was used in 1:1000 dilution. Samples were observed using a confocal microscope (Fluoview, Olympus), and digital images were assembled using Adobe Photoshop. The frozen brains mounted in Tissue-Tek were sectioned in freezing microtome to 20 μM thickness. Sections were fixed with 4% paraformaldehyde in PBS for 20 min, washed several times, blocked with 5% non-fat dried milk for 1 h and then incubated overnight with primary antibody. Staining was carried out using an ABC Elite kit (Vector Laboratories). Dilutions of the different primary antibodies used were the same as described for the immunofluorescence. The frequency of the positively stained NIIs in the R6/1 transgenic mice brain sections were estimated by counting approximately 500 propidium iodide stained nuclei in different parts of the cerebral cortex and striatum.

Assay of proteasome and caspase-3-like protease activity

The HD 16Q and HD 150Q cells were plated in a 6-well tissue cultured plate and on the following day, cells were treated with either dbcAMP alone or dbcAMP and ponasterone A together for different days. Isolated cells at each day were suspended in 100 μl of either proteasome assay buffer (10 mM Tris pH 7.4, 1 mM EDTA, 5 mM ATP, 5 mM DTT and 20% (v/v) glycerol) or caspase 3 assay buffer (10 mM HEPES pH 7.4, 2 mM EDTA, 0.1% CHAPS, 5 mM DTT and 1 mM PMSF), lysed by sonication and then centrifuged at 15 000 *g* for 15 min at 4°C. The supernatant (25 μg) or the pellet (10 μl; after suspension of the total pellet in 100 μl of the respective assay buffer) was incubated either in the proteasome activity assay buffer [50 mM Tris pH 7.4, 0.5 mM EDTA and 50 μM Suc-Leu-Leu-Val-Tyr-MCA (Affinity research product)] or caspase-3-like protease activity assay buffer [20 mM HEPES pH 7.4, 2 mM DTT, 10% (v/v) glycerol and 50 μM Ac-Asp-Glu-Val-Asp-MCA (Peptide Institute)] for different time periods to obtain linearity of the reaction. Protease activities at a particular time point (30 min) within the linear range were used to calculate

the data. The fluorescence intensity was measured at 380 nm excitation and 460 nm emission using a Wallac multi-label counter (Amersham-Pharmacia Biotech). Statistical analysis was performed using the Student's *t*-test and $P < 0.05$ was considered to indicate statistical significance.

Measurement of mitochondrial membrane potential and release of cytochrome c

Neuro2a cells (wild-type) after treatment with 10 μM lactacystin for 48 h or the HD 150Q cell lines after 72 h of differentiation and induction, were incubated with 5 μM JC-1 (5,5′,6,6′-tetrachloro-1,1′,3,3′-tetraethylbenzimidazolocarbocyanine iodide from Molecular Probes) fluorescence dye for 30 min in the CO_2 incubator and washed several times with PBS. Mitochondrial membrane potential was evaluated qualitatively under a confocal microscope. In the lactacystin experiment, both monomer and J-aggregates were excited simultaneously by 488 nm argon-ion laser sources, whereas in all other cases only J-aggregates were selectively excited using 568 nm argon-krypton laser sources.

To investigate the release of cytochrome c from mitochondria, subconfluent cells grown on dishes were treated as indicated in the figure legend. At the end of the treatment, cells were scraped, washed in the PBS, washed in the sucrose buffer (20 mM HEPES pH 7.5, 10 mM KCl, 1.5 mM $MgCl_2$, 1 mM EDTA, 1 mM EGTA, 1 mM DTT and 0.1 mM PMSF containing 250 mM sucrose) and resuspended in the same buffer. After 1 h of incubation on ice, cells were lysed by Dounce homogenizer of B-type pestle with 30 strokes. Homogenates were centrifuged at 750 *g* for 10 min at 4°C, and the supernatants were re-centrifuged at 10 000 *g* for 15 min at 4°C to collect the mitochondrial pellet. The resulting supernatants were again centrifuged at 100 000 *g* for 1 h at 4°C, and the final supernatant used as a cytosolic fraction. Both the mitochondrial and cytosolic fraction were then processed for immunoblotting.

ACKNOWLEDGEMENTS

This work was supported in part by a Grant-in-Aid from the Ministry of Health and Welfare and from the Ministry of Education, Science, Sports and Culture, Japan.

REFERENCES

1. Huntington's Disease Collaborative Research Group (1993) A novel gene containing a trinucleotide repeat that is expanded and unstable on Huntington's disease chromosomes. The Huntington's Disease Collaborative Research Group. *Cell*, **72**, 971–983.
2. Ross, C.A. (1995) When more is less: pathogenesis of glutamine repeat neurodegenerative diseases. *Neuron*, **15**, 493–496.
3. Paulson, H.L. and Fischbeck, K.H. (1996) Trinucleotide repeats in neurogenetic disorders. *Annu. Rev. Neurosci.*, **19**, 79–107.
4. Reddy, P.S. and Housman, D.E. (1997) The complex pathology of trinucleotide repeats. *Curr. Opin. Cell Biol.*, **9**, 364–372.
5. Vonsattel, J.P., Myers, R.H., Stevens, T.J., Ferrante, R.J. and Bird, E.D. (1985) Neuropathological classification of Huntington's disease. *J. Neuropathol. Exp. Neurol.*, **44**, 559–577.
6. Ross, C.A. (1997) Intranuclear neuronal inclusions: a common pathogenic mechanism for glutamine-repeat neurodegenerative diseases? *Neuron*, **19**, 1147–1150.
7. Kim, T.W. and Tanzi, R.E. (1998) Neuronal intranuclear inclusions in polyglutamine diseases: nuclear weapons or nuclear fallout? *Neuron*, **21**, 657–659.
8. Paulson, H.L. (1999) Protein fate in neurodegenerative proteinopathies: polyglutamine diseases join the (mis)fold. *Am. J. Hum. Genet.*, **64**, 339–345.
9. DiFiglia, M., Sapp, E., Chase, K.O., Davies, S.W., Bates, G.P., Vonsattel, J.P. and Aronin, N. (1997) Aggregation of huntingtin in neuronal intranuclear inclusions and dystrophic neurites in brain. *Science*, **277**, 1990–1993.
10. Becher, M.W., Kotzuk, J.A., Sharp, A.H., Davies, S.W., Bates, G.P., Price, D.L. and Ross, C.A. (1998) Intranuclear neuronal inclusions in Huntington's disease and dentatorubral and pallidoluysian atrophy: correlation between the density of inclusions and IT15 CAG triplet repeat length. *Neurobiol. Dis.*, **4**, 387–397.
11. Gutekunst, C.A., Li, S.H., Yi, H., Mulroy, J.S., Kuemmerle, S., Jones, R., Rye, D., Ferrante, R.J., Hersch, S.M. and Li, X.J. (1999) Nuclear and neuropil aggregates in Huntington's disease: relationship to neuropathology. *J. Neurosci.*, **19**, 2522–2534.
12. Davies, S.W., Turmaine, M., Cozens, B.A., DiFiglia, M., Sharp, A.H., Ross, C.A., Scherzinger, E., Wanker, E.E., Mangiarini., L. and Bates, G.P. (1997) Formation of neuronal intranuclear inclusions underlies the neurological dysfunction in mice transgenic for the HD mutation. *Cell*, **90**, 537–548.
13. Martindale, D., Hackam, A., Wieczorek, A., Ellerby, L., Wellington, C., McCutcheon, K., Singaraja, R., Kazemi-Esfarjani, P., Devon, R., Kim, S.U. *et al*. (1998) Length of huntingtin and its polyglutamine tract influences localization and frequency of intracellular aggregates. *Nat. Genet.*, **18**, 150–154.
14. Hackam, A.S., Singaraja, R., Zhang, T., Gan, L. and Hyden, M.R. (1999) *In vitro* evidence for both the nucleus and cytoplasm as subcellular sites of pathogenesis in Huntington's disease. *Hum. Mol. Genet.*, **8**, 25–33.
15. Moulder, K.L., Onodera, O., Burke, J.R., Strittmatter, W.J. and Johnson, E.M.,Jr (1999) Generation of neuronal intranuclear inclusions by polyglutamine-GFP: analysis of inclusion clearance and toxicity as a function of polyglutamine length. *J. Neurosci.*, **19**, 705–715.
16. Li, S.-H., Cheng, A.L., Li, H. and Li, X.-J. (1999) Cellular defects and altered gene expression in PC12 cells stably expressing mutant huntingtin. *J. Neurosci.*, **19**, 5159–5172.
17. Ona, V.O., Li, M., Vonsattel, J.P.G., Andrews, L.J., Khan, S.Q., Chung, W.M., Fre, A.S., Menon, A., Li, X.-J., Stieg, P.E., *et al*. (1999) Inhibition of caspase-1 slows disease progression in a mouse model of Huntington's disease. *Nature*, **399**, 263–267.
18. Chen, M., Ona, V.O., Li, M., Ferrante, R.J., Fink, K.B., Zhu, S., Bian, J., Guo, L., Farrell, L.A., Hersch, S.M. *et al*. (2000) Minocycline inhibits caspase-1 and caspase-3 expression and delays mortality in a transgenic mouse model of Huntington disease. *Nat. Med.*, **6**, 797–801.
19. Sanchez, I., Xu, C.-J., Juo, P., Kakizuka, A., Blenis, J. and Yuan, J. (1999) Caspase-8 is required for cell death induced by expanded polyglutamine repeats. *Neuron*, **22**, 623–633.
20. Sawa, A., Wiegand, G., Cooper, J., Margolis, R.L., Sharp, A.H., Lawler, J.F.,Jr, Greenamyre, T., Snyder, S.H. and Ross, C.A. (1999) Increased apoptosis of Huntington disease lymphoblasts associated with repeat length-dependent mitochondrial depolarization. *Nat. Med.*, **5**, 1194–1198.
21. Cummings, C.J., Mancini, M.A., Antalffy, B., DeFranco, D.B., Orr, H.T. and Zoghbi, H.Y. (1998) Chaperone suppression of aggregation and altered subcellular proteasome localization imply protein misfolding in SCA1. *Nat. Genet.*, **19**, 148–154.
22. Chai, Y., Koppenhafer, S.L., Shoesmith, S.J., Perez, M.K. and Paulson, H.L. (1999) Evidence for proteasome involvement in polyglutamine disease: localization to nuclear inclusions in SCA3/MJD and suppression of polyglutamine aggregation *in vitro*. *Hum. Mol. Genet.*, **8**, 673–682.
23. Chai, Y., Koppenhafer, S.L., Bonini, N.M. and Paulson, H.L. (1999) Analysis of the role of heat shock protein (Hsp) molecular chaperones in polyglutamine disease. *J. Neurosci.*, **19**, 10338–10347.
24. Stenoien, D.L., Cummings, C.J., Adams, H.P., Mancini, M.G., Patel, K., DeMartino, G.N., Marcelli, M., Weigel, N.L. and Mancini, M.A. (1999) Polyglutamine-expanded androgen receptors form aggregates that sequester heat shock proteins, proteasome components and SRC-1, and are suppressed by the HDJ-2 chaperone. *Hum. Mol. Genet.*, **8**, 731–741.
25. Wyttenbach, A., Carmichael, J., Swartz, J., Furlong, R.A., Narain, Y., Rankin, J. and Rubinsztein, D.C. (2000) Effects of heat shock, heat shock protein 40 (HDJ-2), and proteasome inhibition on protein aggregation in cellular models of Huntington's disease. *Proc. Natl Acad. Sci. USA*, **97**, 2898–2903.
26. Cummings, C.J., Reinstein, E., Sun, Y., Antalffy, B., Jiang, Y.-H., Ciechanover, A., Orr, H.T., Beaudet, A.L. and Zoghbi, H. (1999) Mutation of the E6-AP ubiquitin ligase reduces nuclear inclusion frequency while accelerating polyglutamine-induced pathology in SCA1 mice. *Neuron*, **24**, 879–892.

27. Ciechanover, A. (1998) The ubiquitin-proteasome pathway: on protein death and cell life. *EMBO J.*, **17**, 7151–7160.
28. Schwartz, A.L. and Ciechanover, A. (1999) The ubiquitin-proteasome pathway and pathogenesis of human diseases. *Annu. Rev. Med.*, **50**, 57–74.
29. Sadoul, R., Fernandez, P.A., Quiquerez, A.L., Martinou, I., Maki, M., Schroter, M., Becherer, J.D., Irmler, M., Tschopp, J. and Martinou, J.C. (1996) Involvement of the proteasome in the programmed cell death of NGF-deprived sympathetic neurons. *EMBO J.*, **15**, 3845–3852.
30. Drexler, H.C. (1997) Activation of the cell death program by inhibition of proteasome function. *Proc. Natl Acad. Sci. USA*, **94**, 855–860.
31. Lopes, U.G., Erhardt, P., Yao, R. and Cooper, M. (1997) p53-dependent induction of apoptosis by proteasome inhibitors. *J. Biol. Chem.*, **272**, 12893–12896.
32. Qiu, J.H., Asai, A., Chi, S., Saito, N., Hamada, H. and Kirini, T. (2000) Proteasome inhibitors induce cytochrome c-caspase-3-like protease-mediated apoptosis in cultured cortical neurons. *J. Neurosci.*, **20**, 259–265.
33. Drexler, H.C.A., Risau, W. and Konerding, M.A. (2000) Inhibition of proteasome function induces programmed cell death in proliferating endothelial cells. *FASEB J.*, **14**, 65–77.
34. Meriin, A.B., Gabai, V.L., Aglom, J., Shifrin, V.I. and Sherman, M.Y. (1998) Proteasome inhibitors activate stress kinases and induce Hsp72. Diverse effects on apoptosis. *J. Biol. Chem.*, **273**, 6373–6379.
35. Bush, K.T., Goldberg, A.L. and Nigam, S.K. (1997) Proteasome inhibition leads to a heat-shock response, induction of endoplasmic reticulum chaperones, and thermotolerance. *J. Biol. Chem.*, **272**, 9086–9092.
36. Wang, G.H., Mitsui, K., Kotliarova, S., Yamashita, A., Nagao, Y., Tokuhiro, S., Iwatsubo, T., Kanazawa, I. and Nukina, N. (1999) Caspase activation during apoptotic cell death induced by expanded polyglutamine in N2a cells. *Neuroreport*, **10**, 2435–2438.
37. Perutz, M.F., Johnson, T., Suzuki, M. and Finch, J.T. (1994) Glutamine repeats as polar zippers: their possible role in inherited neurodegenerative diseases. *Proc. Natl Acad. Sci. USA*, **91**, 5355–5358.
38. Stoott, K., Blackburn, J.M., Bulter, P.J.G. and Perutz, M.F. (1995) Incorporation of glutamine repeats makes protein oligomerize: implications for neurodegenerative diseases. *Proc. Natl Acad. Sci. USA*, **92**, 6509–6513.
39. Harrison, P.M., Bamborough, P., Daggett, V., Prusiner, S.B. and Cohen, F.E. (1997) The prion folding problem. *Curr. Opin. Struct. Biol.*, **7**, 53–59.
40. Bercovich, B., Stancovsky, I., Mayer, A., Blumenfeld, N., Laszlo, A., Schwartz, A.L. and Ciechanover, A. (1997) Ubiquitin-dependent degradation of certain protein substrates *in vitro* requires the molecular chaperone Hsc70. *J. Biol. Chem.*, **272**, 9002–9010.
41. Levitskaya, J., Sharipo, A., Leonchiks, A., Ciechanover, A. and Masucci, M.G. (1997) Inhibition of ubiquitin/proteasome-dependent protein degradation by the Gly-Ala repeat domain of the Epstein–Barr virus nuclear antigen 1. *Proc. Natl Acad. Sci. USA*, **94**, 12616–12621.
42. Sharipo, A., Imreh, M., Leonchiks, A., Imreh, S. and Masucci, M.G. (1998) A minimal glycine-alanine repeat prevents the interaction of ubiquitinated I κB α with the proteasome: a new mechanism for selective inhibition of proteolysis. *Nat. Med.*, **4**, 939–944.
43. Saudou, F., Finkbeiner, S., Devys, D. and Greenberg, M.E. (1998) Huntingtin acts in the nucleus to induce apoptosis but death does not correlate with the formation of intranuclear inclusions. *Cell*, **95**, 55–66.
44. Jiang, Y.-H., Armstrong, A., Albrecht, U., Atkins, C.M., Noebels, J.L., Eichele, G., Sweatt, J.D. and Beaudet, A.L. (1998) Mutation of the angelman ubiquitin ligase in mice causes increased cytoplasmic p53 and deficits of contextual learning and long-term potentiation. *Neuron*, **21**, 799–811.
45. Fisher, D.F. (1994) Apoptosis in cancer therapy: crossing the threshold. *Cell*, **78**, 539–542.
46. Li, B. and Dou, Q.P. (2000) Bax degradation by the ubiquitin/proteasome-dependent pathway: involvement in tumor survival and progression. *Proc. Natl Acad. Sci. USA*, **97**, 3850–3855.
47. Schuler, M., Bossy-Wetzel, E., Goldstein, J.C., Fitzgerald, P. and Green, D.R. (2000) p53 induces apoptosis by caspase activation through mitochondrial cytochrome c release. *J. Biol. Chem.*, **275**, 7337–7342.
48. Kluck, R.M., Esposti, M.D., Perkins, G., Renken, C., Kuwana, T., Bossy-Wetzel, E., Goldberg, M., Allen, T., Barber, M.J., Green D.R. and Newmeyer, D.D. (1999) The pro-apoptotic proteins, Bid and Bax, cause a limited permeabilization of the mitochondrial outer membrane that is enhanced by cytosol. *J. Cell Biol.*, **147**, 809–822.
49. Green, D.R. and Reed, J.C. (1998) Mitochondria and apoptosis. *Science*, **281**, 1309–1312.
50. Kuida, K., Hayder, T.F., Kuan, C.Y., Gu, Y., Taa, C., Karasuyama, H., Su, M.S., Rakic, P. and Flavel, R.A. (1998) Reduced apoptosis and cytochrome c-mediated caspase activation in mice lacking caspase 9. *Cell*, **94**, 325–337.
51. Nicholson, D.W. and Thornberry, N.A. (1997) Caspases: killer proteases. *Trends Biochem. Sci.*, **22**, 299–306.
52. Gu, M., Gash, M., Mann, V.M., Javoy-Agid, F., Cooper, J.M. and Schapira, A.H. (1996) Mitochondrial defect in Huntington's disease caudate nucleus. *Ann. Neurol.*, **39**, 385–389.
53. Koroshetz, W.J., Jenkins, B.G., Rosen, B.R. and Beal, M.F. (1997) Energy metabolism defects in Huntington's disease and effects of coenzyme Q10. *Ann. Neurol.*, **41**, 160–165.
54. Steffan, J.S., Kazantsev, A., Boskovic, O.S., Greenwald, M., Zhu, Y.-Z., Gohler, H., Wanker, E.E., Bates, G.P., Housman, D.E. and Thompson, L.M. (2000) The Huntington's disease protein interacts with p53 and CREB-binding protein and represses transcription. *Proc. Natl Acad. Sci. USA*, **97**, 6763–6768.
55. Reddy, P.H., Williams, M., Charles, V., Garrett, L., Pike-Buchanan, L., Whetsell, W.O.,Jr, Miller, G. and Tagle, D.A. (1998) Behavioural abnormalities and selective neuronal loss in HD transgenic mice expressing mutated full-length HD cDNA. *Nat. Genet.*, **20**, 198–202.
56. Mangiarini, L., Sathasivam, K., Seller, M., Cozens, B., Harper, A., Hetherington, C., Lawton, M., Trottier, Y., Lehrach, H., Davies, S.W. and Bates, G.P. (1996) Exon 1 of the HD gene with an expanded CAG repeat is sufficient to cause a progressive neurological phenotype in transgenic mice. *Cell*, **87**, 493–506.
57. Turmaine, M., Raza, A., Mahal, A., Mangiarini, L., Bates, G.P. and Davies, S.W. (2000) Nonapoptotic neurodegeneration in a transgenic mouse model of Huntington's disease. *Proc. Natl Acad. Sci. USA*, **97**, 8093–8097.
58. Ferrabte, R., Anderson, O.A., Jenkins, B.G., Dedeoglu, A., Kuemmerle, A., Kubilus, J.K., Kaddurah-Daouk, R., Hersch, S.M. and Beal, M.F. (2000) Neuroprotective effects of creatine in a transgenic mouse model of Huntington's disease. *J. Neurosci.*, **20**, 4389–4397.
59. Perez, M.K., Paulson, H.L., Pendse, S.J., Saionz, S.J., Bonini, N.M. and Pittman, R.N. (1998) Recruitment and the role of nuclear localization in polyglutamine-mediated aggregation. *J. Cell Biol.*, **143**, 1457–1470.
60. Kazantsev, A., Preisinger, E., Dranovsky, A., Goldgaber, D. and Housman, D. (1999) Insoluble detergent-resistant aggregates form between pathological and nonpathological lengths of polyglutamine in mammalian cells. *Proc. Natl Acad. Sci. USA*, **96**, 11404–11409.
61. Boutell, J.M., Thomas, P., Neal, J.W., Weston, V.J., Duce, J., Harpar, P.S. and Jones, A.L. (1999) Aberrant interactions of transcriptional repressor proteins with the Huntington's disease gene product, huntingtin. *Hum. Mol. Genet.*, **8**, 1647–1655.
62. Obin, M., Mesco, E., Gong, X., Haas, A.L., Joseph, J. and Taylor, A. (1998) Neurite outgrowth in PC12 cells. Distinguishing the roles of ubiquitylation and ubiquitin-dependent proteolysis. *J. Biol. Chem.*, **274**, 11789–11795.
63. Giasson, B.I., Bruening, W., Durham, H.D. and Mushynski, W.E. (1999) Activation of stress-activated protein kinases correlates with neurite outgrowth induced by protease inhibition in PC12 cells. *J. Neurochem.*, **72**, 1081–1087.
64. Liu, F.Y. (1998) Expression of polyglutamine-expanded Huntingtin activates the SEK1-JNK pathway and induces apoptosis in a hippocampal neuronal cell line. *J. Biol. Chem.*, **273**, 28873–28877.
65. Yasuda, S., Inoue, K., Hirabayashi, M., Higashiyama, H., Yamamoto, Y., Fuyuhiro, H., Komure, O., Tanaka, F., Sobue, G., Tsuchiya, K. *et al.* (1999) Triggering of neuronal cell death by accumulation of activated SEK1 on nuclear polyglutamine aggregations in PML bodies. *Genes Cell*, **4**, 743–756.